


## Article

# The Steric Effect in Preparations of Vanadium(II)/(III) Dinitrogen Complexes of Triamidoamine Ligands Bearing Bulky Substituents

 Yoshiaki Kokubo <sup>1</sup>, Itsuki Igarashi <sup>2</sup>, Kenichi Nakao <sup>2</sup>, Wataru Hachiya <sup>2</sup>, Shinichi Kugimiya <sup>1</sup>, Tomohiro Ozawa <sup>2</sup>, Hideki Masuda <sup>1,2</sup>  and Yuji Kajita <sup>1,\*</sup> 
<sup>1</sup> Faculty of Engineering, Aichi Institute of Technology, 1247 Yachigusa, Yakusa-cho, Toyota 470-0392, Japan

<sup>2</sup> Graduate School of Engineering, Nagoya Institute of Technology, Gokiso-cho, Showa-ku, Nagoya 466-8555, Japan

\* Correspondence: ykaji1974@aitech.ac.jp

**Abstract:** The reactions of newly designed lithiated triamidoamines  $\text{Li}_3\text{L}^{\text{R}}$  ( $\text{R} = \text{iPr}$ , Pen, and  $\text{Cy}_2$ ) with  $\text{VCl}_3(\text{THF})_3$  under  $\text{N}_2$  yielded dinitrogen–divanadium complexes with a  $\mu\text{-N}_2$  between vanadium atoms  $[\{\text{V}(\text{L}^{\text{R}})\}_2(\mu\text{-N}_2)]$  ( $\text{R} = \text{iPr}$  (**1**) and Pen (**2**)) for the former two, while not dinitrogen–divanadium complexes but a mononuclear vanadium complex with a vacant site,  $[\text{V}(\text{L}^{\text{Cy}_2})]$  ( $\text{R} = \text{Cy}_2$  (**3**)), were obtained for the third ligand. The V–N<sub>N2</sub> and N–N distances were 1.7655(18) and 1.219(4) Å for **1** and 1.7935(14) and 1.226(3) Å for **2**, respectively. The  $\nu(^{14}\text{N}\text{--}^{14}\text{N})$  stretching vibrations of **1** and **2**, as measured using resonance Raman spectroscopy, were detected at 1436 and 1412  $\text{cm}^{-1}$ , respectively. Complex **3** reacted with potassium metal in the presence of 18-crown-6-ether under  $\text{N}_2$  to give a heterodinuclear vanadium complex with  $\mu\text{-N}_2$  between vanadium and potassium,  $[\text{VK}(\text{L}^{\text{Cy}_2})(\mu\text{-N}_2)(18\text{-crown-6})]$  (**4**). The N–N distance and  $\nu(^{14}\text{N}\text{--}^{14}\text{N})$  stretching for **4** were 1.152(3) Å and 1818  $\text{cm}^{-1}$ , respectively, suggesting that **4** is more activated than complexes **1** and **2**. The complexes **1**, **2**, **3**, and **4** reacted with HOTf and  $\text{K}[\text{C}_{10}\text{H}_8]$  to give  $\text{NH}_3$  and  $\text{N}_2\text{H}_4$ . The yields of  $\text{NH}_3$  and  $\text{N}_2\text{H}_4$  (per V atom) were 47 and 11% for **1**, 38 and 16% for **2**, 77 and 7% for **3**, and 80 and 5% for **4**, respectively, and **3** and **4**, which have a ligand  $\text{L}^{\text{Cy}_2}$ , showed higher reactivity than **1** and **2**.

**Keywords:** dinitrogen complex; vanadium; bulky substituents; dinitrogen activation; steric effect; triamidoamine ligand



**Citation:** Kokubo, Y.; Igarashi, I.; Nakao, K.; Hachiya, W.; Kugimiya, S.; Ozawa, T.; Masuda, H.; Kajita, Y. The Steric Effect in Preparations of Vanadium(II)/(III) Dinitrogen Complexes of Triamidoamine Ligands Bearing Bulky Substituents. *Molecules* **2022**, *27*, 5864. <https://doi.org/10.3390/molecules27185864>

Academic Editor: Carlo Santini

Received: 24 August 2022

Accepted: 7 September 2022

Published: 9 September 2022

**Publisher's Note:** MDPI stays neutral with regard to jurisdictional claims in published maps and institutional affiliations.



**Copyright:** © 2022 by the authors. Licensee MDPI, Basel, Switzerland. This article is an open access article distributed under the terms and conditions of the Creative Commons Attribution (CC BY) license (<https://creativecommons.org/licenses/by/4.0/>).

## 1. Introduction

Dinitrogen activation using vanadium ions has been intensely investigated by bioinorganic chemists and coordination chemists in order to understand the role of vanadium ions as an important factor in vanadium nitrogenase enzymes [1–9]. Most of the dinitrogen–vanadium complexes studied are dinuclear complexes with a  $\mu\text{-N}_2$  ligand in the end-on mode [10]. On the other hand, mononuclear vanadium–dinitrogen complexes are scarce [11–14]. It has also been previously reported that some dinitrogen–vanadium complexes produce ammonia and hydrazine [15–22]. Recently, dinitrogen–vanadium complexes, which are supported with anionic pyrrole-based PNP-type pincer and aryloxy ligands, have been successfully used for catalytic dinitrogen reduction by a group of Nishibayashi [20].

Triamidoamine (tris(2-amidoethyl)amine) ligands are very useful ligands that bind as multidentate ligands when forming metal complexes, creating binding sites for external ligands on the axis. Therefore, many complexes with the ligands have been investigated [14,21–43]. Schrock and co-workers reported the molybdenum complex with the triamidoamine ligand with a very bulky substituent group, HIPT (3,5-(2,4,6- $\text{iPr}_3\text{C}_6\text{H}_2$ )<sub>2</sub> $\text{C}_6\text{H}_3$ ) [37]. This molybdenum complex is the first example of catalytic ammonia production [38]. In this complex, the HIPT group functioned to inhibit dimerization of the molybdenum center and provide a pocket for

binding an external ligand, such as  $N_2$ , HNN,  $H_2NN$ , NH,  $NH_3$ , N, NO, THF, CO, S,  $Me_3SiN$ , and so on [14,37,39,40]. Additionally, they also argued that the  $N_2$  ligand is protonated in the distal pathway by steric hindrance of the HIPT group [39]. On the other hand, dinuclear dinitrogen–molybdenum complexes with triamidoamine ligands have also been studied, but the substituents of these triamidoamine ligands are smaller than HIPT, such as TMS, aryl, and alkyl groups [21,22,41–44], and those with larger substituents have not been studied.

We have previously reported the syntheses and crystal structures of the dinitrogen–divanadium complexes bearing a triamidoamine ligand with a secondary C atom on the terminal N atom [ $\{V(L^R)\}_2(\mu-N_2)$ ] ( $R = iBu, EtBu, iPr_2Bn, Bn, MeBn$ ) and studied the conversion of the bridging  $N_2$  ligand to ammonia using these complexes in the presence of proton sources (HOTf, [LutH](OTf)) and reductants ( $M^+[C_{10}H_8]^-$   $M = K$  or  $Na$ ) [21,22]. Furthermore, the crystal structure and protonation reaction of its  $Na^+$  adduct ( $[Na\{V(L^{iBu})\}_2(\mu-N_2)]$ ) were also studied (Figure 1) [22]. By introducing a secondary carbon atom on the terminal nitrogen atom of the triamidoamine ligand, these dinitrogen complexes can easily form dimer structures because the steric hindrance around the vanadium ion is smaller than those modified with bulky silyl or aryl groups. Therefore, we considered it would be possible to systematically investigate the structure and reactivity of mononuclear or dinuclear dinitrogen complexes using a series of triamidoamine ligands with different steric hindrances. The space-filling models of previously reported divanadium–dinitrogen complexes [ $\{V(L^R)\}_2(\mu-N_2)$ ] ( $R = iBu$  and  $MeBn$ ) are shown in Figure 1. In these complexes, there is no space around the secondary carbon atom (red), suggesting that a tertiary carbon atom was introduced on the terminal N atom to form a mononuclear vanadium–dinitrogen complex. If mononuclear and dinuclear complexes can be synthesized using triamidoamine ligands with the same backbone, meaningful comparisons can be made regarding their structures and reactivities in dinitrogen activation.

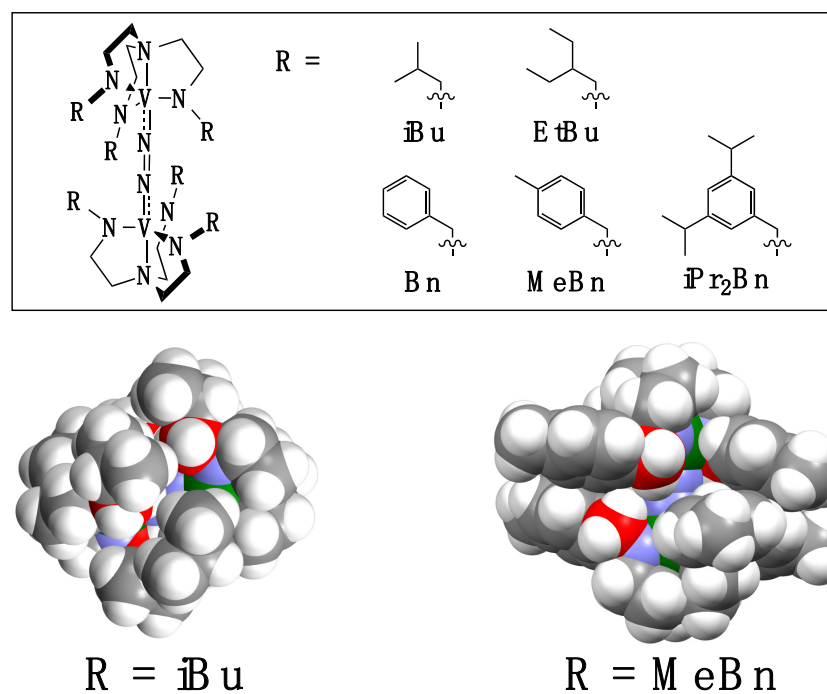


**Figure 1.** The structures of our previously reported divanadium–dinitrogen complexes [ $\{V(L^R)\}_2(\mu-N_2)$ ] (**top**) and space-filling models of two dinitrogen complexes [ $\{V(L^R)\}_2(\mu-N_2)$ ] ( $R = iBu$  and  $MeBn$ ) (**bottom**). The hydrogen, nitrogen, and vanadium atoms are shown in white, blue, and green, respectively. Secondary carbon atoms on the terminal N atoms are red, and the other carbon atoms are gray.

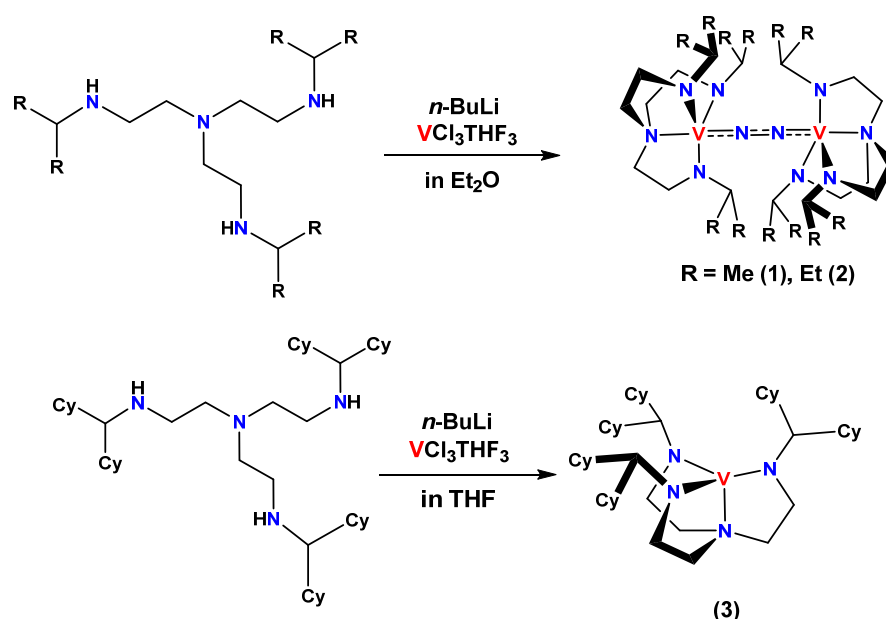
In this study, three vanadium complexes with a series of triamidoamine ligands bearing bulky substituents were synthesized under  $N_2$  atmosphere, and the characterizations, crystal structures, and protonation reactivities of the obtained complexes were investigated, compared, and discussed with those previously reported.

## 2. Results and Discussion

### 2.1. Syntheses of Ligands and Their Vanadium Complexes 1, 2, and 3

Three types of tren derivatives  $H_3L^R$  ( $R = iPr$  (tris(2-isopropylaminoethyl)amine,  $H_3L^{iPr}$ ), Pen (tris(2-(3-pentylamino)ethyl)amine,  $H_3L^{Pen}$ ), and  $Cy_2$  (tris(2-dicyclohexylmethylaminoethyl)amine,  $H_3L^{Cy_2}$ )) were prepared using previously reported methods [21,22].  $H_3L^{iPr}$  and  $H_3L^{Pen}$  were obtained as light-yellow oil and  $H_3L^{Cy_2}$  as colorless crystals, which were characterized using  $^1H$  NMR,  $^{13}C$  NMR, and IR spectroscopic methods. The  $H_3L^R$  was deprotonated and used as a triamidoamine ligand for the synthesis of dinitrogen complexes.

The reactions of lithiated triamidoamines  $Li_3L^R$  ( $R = iPr$ , Pen, and  $Cy_2$ ) with  $VCl_3(THF)_3$  at room temperature under  $N_2$  produced dinitrogen–divanadium complexes  $[V(L^R)]_2(\mu-N_2)$  ( $R = iPr$  (1) and Pen (2)) for the former two. On the other hand, for the third ligand, a mononuclear vanadium complex  $[V(L^{Cy_2})]$  (3) was obtained instead of a dinitrogen–divanadium complex (Scheme 1). When all complex solutions were left at room temperature for several days, single crystals of complexes 1 and 3 were obtained as dark green crystals, and that of complex 2 was observed as dark purple crystals. These complexes were stable at low temperature under  $N_2$  atmosphere but decomposed under air atmosphere.



**Scheme 1.** Syntheses of 1, 2, and 3.

### 2.2. Crystal Structures of 1 and 2

The crystal structures of 1 and 2 are shown in Figure 2, and the crystal parameters are listed together in Tables 1 and S1. Complexes 1 and 2 were expected to be mononuclear vanadium complexes because of their bulky substituents, but they turned out to be dinuclear vanadium complexes with bridging dinitrogen in the end-on mode. The coordination geometries around the vanadium centers in 1 and 2 are a nearly undistorted triangular bipyramid ( $\tau = 1.0$  and  $1.0$ , respectively) (Figure 2), where 1 is a perfect trigonal bipyramidal geometry, 0 is a perfect square pyramidal geometry [45]. The N–N bond lengths for 1 and 2 are 1.219(4) and 1.226(3) Å, respectively, and that of complex 2 are slightly longer than those of 1 and the previously reported divanadium–dinitrogen complexes [21,22]. The bond lengths around the vanadium center in 2 ( $V-N_{N_2}$  (1.7935(14) Å),  $V-N_{amido}$  (1.9276(16), 1.9284(16), 1.9234(16) Å), and  $V-N_{amine}$  (2.1854(16) Å)) are also more elongated than those

of **1** ( $V-N_{N_2}$  (1.7647(18) Å),  $V-N_{\text{amido}}$  (1.896(2), 1.9123(14), 1.9123(14) Å), and  $V-N_{\text{amine}}$  (2.173(2) Å)). This may also be due to the greater steric repulsion between the alkyl substituents on the N atoms of the triamidoamine ligand in **2** than in **1**. Comparing the space-filling model of **2** with that of **1**, it is obvious that the pentyl group in **2** surrounds the vanadium center more than the isopropyl group in **1** (Figure 3). Thus, it appears that all bond lengths are extended to maintain the dimeric structure, overcoming the pull away to the mononuclear vanadium complex. In fact, the  $V\cdots V$  distances and the distances of the vanadium ion from the plane decided by three  $N_{\text{amido}}$  atoms are 4.7482(8) and 0.3055(12) Å for **1** and 4.8128(7) and 0.3495(10) Å for **2**, respectively, making them longer for complex **2** than for complex **1**. This finding appears to be due to the strong attraction of vanadium ions in complex **2** to the  $\mu-N_2$  ligand.

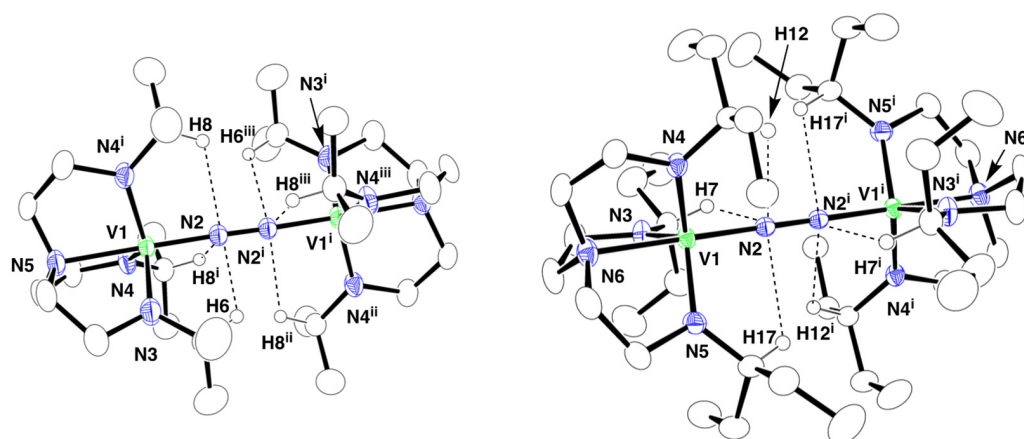


**Figure 2.** X-ray structures of **1** (left) and **2** (right) with the atom numbering scheme (50% probability thermal ellipsoids). Hydrogen atoms except for the hydrogen on the methine carbons and disordered atoms are omitted for clarity. The atoms with superscripts i, ii, and iii in structure of **1** are related to the atoms without them by symmetry operations  $(x, 1 - y, 1 - z)$ ,  $(1 - x, 1 - y, 1 - z)$ , and  $(x, 1 - y, -z)$ , respectively. The atoms with and without superscript i in the structure of **2** are related to each other by symmetry operation  $(1/2 - x, 3/2 - y, 1 - z)$ .

**Table 1.** Selected bond lengths (Å) and angles (deg) for **1** and **2**.

<b>1</b> [a]					
V1–N2	1.7647(18)	V1–N3	1.896(2)	V1–N4	1.9123(14)
V1–N4 <sup>i</sup>	1.9123(14)	V1–N5	2.173(2)	N2–N2 <sup>i</sup>	1.219(4)
$V\cdots V^i$	4.7482(8)	-	-	-	-
N2–V1–N5	178.98(9)	N2 <sup>i</sup> –N2–V1	178.1(3)	N2–V1–N3	98.08(9)
N2–V1–N4	99.78(5)	N2–V1–N4 <sup>i</sup>	99.78(5)	N3–V1–N4	116.68(5)
N3–V1–N4 <sup>i</sup>	116.68(5)	N4–V1–N4 <sup>i</sup>	119.08(10)	-	-
<b>2</b> [b]					
V1–N2	1.7935(14)	V1–N3	1.9276(16)	V1–N4	1.9284(16)
V1–N5	1.9234(16)	V1–N6	2.1854(16)	N2–N2 <sup>i</sup>	1.226(3)
$V\cdots V^i$	4.8128(7)	-	-	-	-
N2–V1–N3	101.91(7)	N2–V1–N4	100.01(7)	N2–V1–N5	99.43(6)
N2–V1–N6	177.75(7)	N3–V1–N4	116.88(7)	N3–V1–N5	116.43(7)
N3–V1–N6	80.34(6)	N4–V1–N5	117.04(7)	N4–V1–N6	78.74(6)
N5–V1–N6	79.57(6)	N2 <sup>i</sup> –N2–V1	177.80(19)	-	-

[a] The atoms with and without superscript i in structure of **1** are related to each other by symmetry operation  $(x, 1 - y, 1 - z)$ . [b] The atoms with and without superscript i in structure of **2** are related to each other by symmetry operation  $(1/2 - x, 3/2 - y, 1 - z)$ .

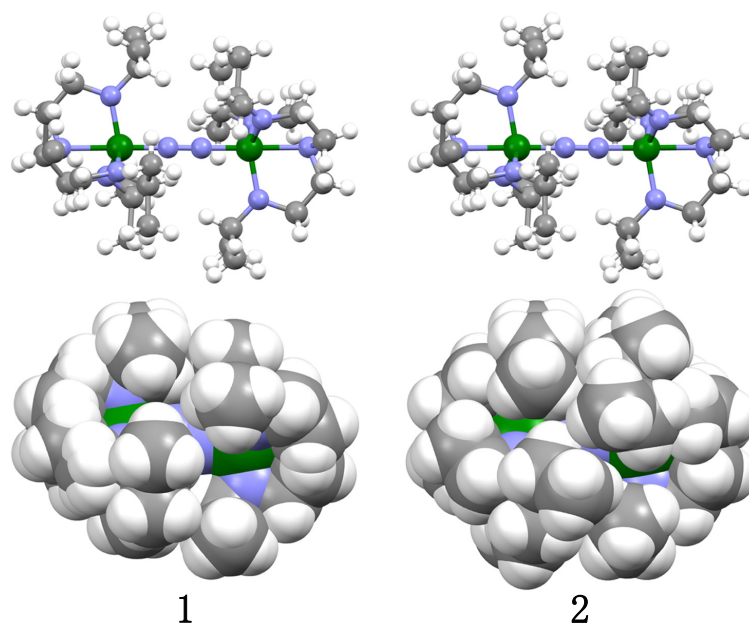


**Figure 3.** Ball and stick (**top**) and space-filling models (**bottom**) of **1** (left side) and **2** (right side).

The  $\mu$ -N<sub>2</sub> ligands in **1** and **2** are stabilized by hydrogen bonding interactions between the N<sub>2</sub> ligand and the methine hydrogen atoms on the N atoms (CH $\cdots$ N<sub>N2</sub> = av. 2.488 Å for **1**, av. 2.611 Å for **2**). This interaction may also contribute to the formation of dimer structures.

### 2.3. Crystal Structure of **3**

The crystal structure of complex **3** is shown in Figure 4, and the crystal parameters are listed in Table 2 and Table S1, respectively. Complex **3**, unlike **1** and **2**, was a mononuclear vanadium complex with no dinitrogen coordination. The geometry around the vanadium center is a trigonal pyramid, with a vacancy on the opposite side of N<sub>amine</sub> (N5) in [L<sup>Cy2</sup>]<sup>3-</sup>. The V1–N3 (1.9433(12) Å) and V1–N4 bonds (1.9593(12) Å) are longer than the V1–N2 bond (1.9281(13) Å) because the steric repulsions between the cyclohexane rings of the dicyclohexylmethyl group on the N2 atom and those on the N3 and N4 atoms are weakened by the overhang of those on the N2 atom attached to the V center. The averaged V–N<sub>amido</sub> bond length in **3** (1.9436 Å) is longer than that of the related triamidoamine–vanadium complex, [V(*t*BuMe<sub>2</sub>SiN)<sub>3</sub>N] (V–N<sub>amido</sub> = 1.930(av.) Å) [26]. This fact indicates that the dicyclohexylmethyl group of **3** leads greater steric repulsion than the *t*BuMe<sub>2</sub>Si group.

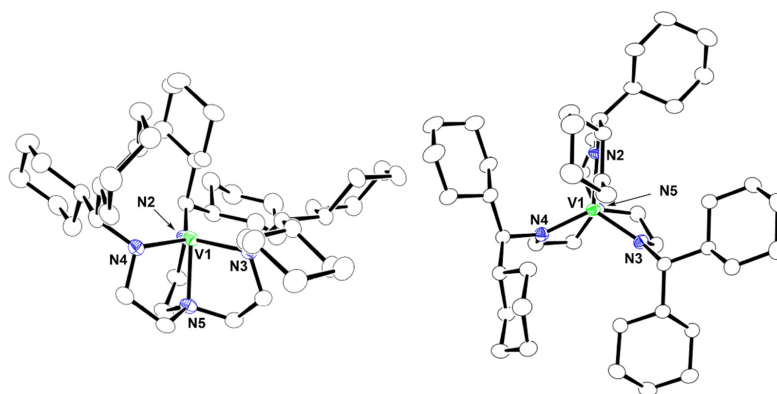


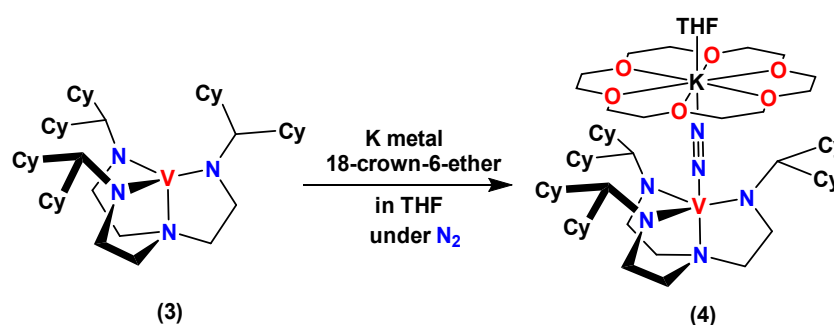
**Figure 4.** Side (**left**) and top (**right**) views of X-ray structure of **3** with the numbering scheme (50% probability thermal ellipsoids). Hydrogen atoms were omitted for clarity.

**Table 2.** Selected bond lengths (Å) and angles (deg) for **3** and **4**.

3					
V1–N2	1.9281 (13)	V1–N3	1.9433 (12)	V1–N4	1.9593 (12)
V1–N5	2.0687 (13)	-	-	-	-
N2–V1–N3	119.11 (6)	N2–V1–N4	118.23 (5)	N2–V1–N5	84.13 (5)
N3–V1–N4	119.29 (5)	N3–V1–N5	83.35 (5)	N4–V1–N5	84.17 (5)
4					
V1–N3	1.853 (3)	V1–N5	1.965 (2)	V1–N6	1.960 (2)
V1–N7	1.955 (2)	V1–N8	2.172 (2)	N3–N4	1.152 (3)
N4–K2	2.648 (3)	-	-	-	-
N8–V1–N3	179.07 (10)	V1–N3–N4	179.08 (3)	N3–N4–K2	173.3 (2)
N5–V1–N6	118.34 (10)	N6–V1–N7	118.80 (10)	N7–V1–N5	116.46 (10)
N5–V1–N8	81.59 (9)	N6–V1–N8	81.40 (10)	N7–V1–N8	81.59 (9)

#### 2.4. Synthesis and Crystal Structure of **4**

The crystal structure of **3** shows that there is an open site on the vanadium ion. Therefore, we attempted to synthesize the N<sub>2</sub> adduct by reacting **3** with potassium metal under N<sub>2</sub> in the presence of 18-crown-6-ether (Scheme 2). Fortunately, a single crystal of the N<sub>2</sub> adduct (**4**) was obtained as green crystals using recrystallization from THF/hexane at −35 °C. Complex **4** gradually decomposed at room temperature even under inert gas (N<sub>2</sub> or Ar).

**Scheme 2.** Synthesis of **4**.

The crystal structure of **4** is shown in Figure 5, and the crystal parameters are listed in Table 2 and Table S1, respectively. Complex **4** had a bridging dinitrogen ligand between the vanadium(II) ion and potassium ion in the end-on mode, the coordination geometry around the vanadium center was trigonal bipyramidal, and the THF molecule coordinated to the potassium ion from the opposite side of the N<sub>2</sub> ligand. The N–N and V–N<sub>N2</sub> bond lengths of **4** are 1.152 (3) and 1.853 (3) Å, respectively. The average of three V–N<sub>amido</sub> bond lengths was found to be 1.960 Å, which is more elongated than those of **3** (1.9436 (av.) Å). This is thought to be due to the increased steric repulsion between the dicyclohexylmethyl groups as a result of the increased ionic radius of the vanadium ion due to the reduction in V(III) to V(II) and the incorporation of the N<sub>2</sub> ligand in the axial position. The N<sub>2</sub> ligand of **4** was also stabilized by hydrogen bonding interactions between the methine proton and the N3 atom of dinitrogen (CH•••N3(N<sub>2</sub>) = av. 2.596 Å). The distance between the mean plane decided by three N<sub>amido</sub> atoms and the vanadium ion (V1 atom) was 0.2888(14) Å, which is smaller than those of **1** and **2**. The space-filling model of **4** is shown in Figure 5 (right). It is clear from this figure that the dicyclohexylmethyl group surrounds not only the α-nitrogen but also the β-nitrogen, suggesting that the dinitrogen–vanadium complex with [L<sup>Cy2</sup>]<sup>3-</sup> ligand is too large to form a dimer structure.



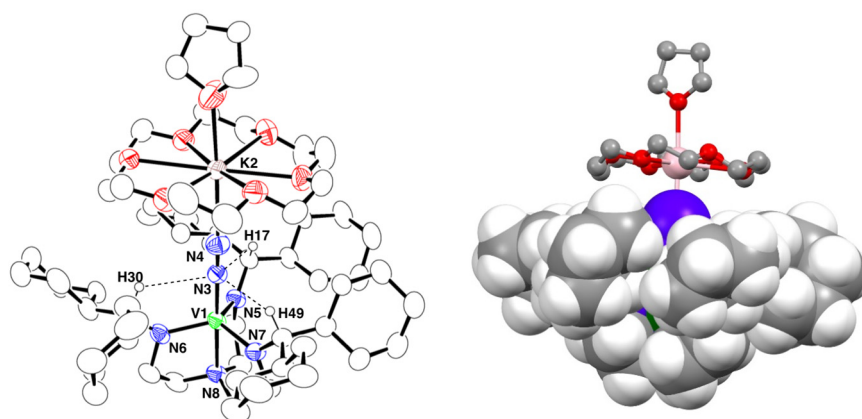


**Figure 5.** (Left) X-ray structure of **4** with the atom numbering scheme (50% probability thermal ellipsoids). The hydrogen atoms, except for the hydrogen on the methine carbons neighboring on the terminal N atoms of the triamidoamine ligand, disordered atoms, and crystal solvates are omitted for clarity. (Right) Side view of space-filling model of **4**. The hydrogen atoms of THF and 18-crown-6-ether are omitted, and the potassium ion, 18-crown-6-ether, and THF are shown in ball and stick model for clarity (C, H, N, O, K, and V are shown in gray, white, blue, red, pink, and green colors, respectively).

### 2.5. Raman and Infrared Spectra of **1**, **2**, and **4**

The  $\nu(^{14}\text{N}\text{--}^{14}\text{N})$  stretching vibrations of **1** and **2** were detected at 1436 and 1412  $\text{cm}^{-1}$  using resonance Raman spectroscopic measurements, respectively (Figures S1 and S2).  $^{15}\text{N}$ -labeled **1** (**1'**) and **2** (**2'**) were both split by a Fermi doublet to show peaks at 1399, 1337  $\text{cm}^{-1}$  and 1380, 1335  $\text{cm}^{-1}$ , respectively. The  $\nu(\text{V}\text{--}^{14}\text{N})$  stretching vibrations of **1** and **2** were observed at 796 and 728  $\text{cm}^{-1}$  from the IR spectra, respectively (Figures S3 and S4). The  $\nu(^{14}\text{N}\text{--}^{14}\text{N})$  and  $\nu(\text{V}\text{--}^{14}\text{N})$  values of **1** are larger than those of **2**, which are in good agreement with the N–N and V–N<sub>N2</sub> bond lengths trends for **1** and **2**. However, these  $\nu(^{14}\text{N}\text{--}^{14}\text{N})$  values are larger than those of previously reported divanadium–dinitrogen complexes (1394–1402  $\text{cm}^{-1}$ ), even though **1** and **2** have longer N–N bonds than those of previously reported divanadium–dinitrogen complexes (1.200 (5)–1.226 (3) Å) [21,22]. Such inversions in bond lengths and vibrational spectra are sometimes observed in the activation chemistry of dinitrogen with transition metals [46].

In the IR spectral measurements, the  $\nu(^{14}\text{N}\text{--}^{14}\text{N})$  peaks for **4** were observed as two bands at 1830 and 1818  $\text{cm}^{-1}$ , which were shifted to 1768 and 1759  $\text{cm}^{-1}$  when  $^{15}\text{N}_2$  was used in the place of  $^{14}\text{N}_2$  (Figure S5). The IR bands at 1830 and 1768  $\text{cm}^{-1}$  were assigned as overtones of the 910 and 885  $\text{cm}^{-1}$ , respectively. When  $^{15}\text{N}$ -labeled **4** (**4'**) was dissolved in THF at room temperature and recrystallized under  $^{14}\text{N}_2$ , the  $\nu(^{14}\text{N}\text{--}^{14}\text{N})$  stretching vibration was observed. This means that the N<sub>2</sub> ligand of **4** is easily exchanged in THF because of the weak V–N<sub>N2</sub> bond.

### 2.6. $^1\text{H}$ -, $^{15}\text{N}$ -, and $^{51}\text{V}$ -NMR Spectra

$^1\text{H}$  NMR spectra of **1** and **2** exhibited sharp peaks in the diamagnetic region, as shown in Figures S6 and S7, respectively. The methine peak of **2** (4.77 ppm) was observed in a higher magnetic field region than that of **1** (5.27 ppm).  $^{15}\text{N}$  NMR spectra of **1** and **2** with  $^{15}\text{N}$ -labeled N<sub>2</sub> were detected at 25.2 and 41.6 ppm (Figures S8 and S9), and  $^{51}\text{V}$  NMR spectra of **1** and **2** were observed at –211 and –47.6 ppm, respectively (Figures S10 and S11). The peaks of **2** were both observed in a lower magnetic field region than those in **1** and our previously reported divanadium–dinitrogen complexes ( $^{15}\text{N}$  NMR: 25.2–33.4 ppm,  $^{51}\text{V}$  NMR: –240.2–143.8 ppm) [21,22]. These findings indicate that the electron densities on the N atoms of dinitrogen and the V atom in **2** are lower than those of complex **1** and the previously reported divanadium–dinitrogen complexes because the electron donation from N<sub>amido</sub> atoms to the V atom in **2** was smaller than those complexes. These facts correspond

well with the result that the V–N<sub>amide</sub> bond length is the longest among the dinuclear vanadium–dinitrogen complexes with triamidoamine ligands reported so far [21,22], due to the large steric repulsion between the pentyl groups. On the other hand, the <sup>1</sup>H NMR spectrum of **3** gave a broadened paramagnetic peak at 915 ppm in the lower magnetic field region (Figure S12) and that of **4** showed broad peaks at 10.2, 3.28, 0.32, 0.08, –0.28, –0.75, –0.95, –1.63, –15.2, and –30.5 ppm in the diamagnetic to higher magnetic field region (Figure S13). The spectrum of **4** includes not only **4** but also solvents (*n*-hexane, THF) and a free ligand, H<sub>3</sub>L<sup>Cy2</sup> (Figure S14). It is thought that the free ligand was probably produced by the decomposition of **4** due to its low thermal stability at room temperature. Unfortunately, we were unable to characterize the products containing vanadium(II) ions produced in the decomposition of **4**. The effective magnetic moment ( $\mu_{\text{eff}}$ ) of **3** was 2.73  $\mu_{\text{B}}$  at 298 K as determined by Evans's NMR solution method [47,48], which indicates that the spin state of **3** is  $S = 1$ . Similarly,  $\mu_{\text{eff}}$  of **4** was estimated to be 1.76  $\mu_{\text{B}}$  at 298 K, indicating that the spin state of **4** is  $S = 1/2$ . These spin states correspond well with the structural findings that complex **3** is a mononuclear vanadium(III) complex with a vacant site, [V(L<sup>Cy2</sup>)], and complex **4** is a hetero-dinuclear vanadium(II) complex with  $\mu$ -N<sub>2</sub> between vanadium and potassium, [VK(L<sup>Cy2</sup>)( $\mu$ -N<sub>2</sub>)(18-crown-6)].

### 2.7. Protonation of 1–4 in the Presence of Reductants

Protonation of **1**, **2**, **3**, and **4** was carried out with a reductant (M[C<sub>10</sub>H<sub>8</sub>] (M = Na<sup>+</sup> or K<sup>+</sup>)) and an acid (HOTf) in THF at –78 °C. The previously reported protonation of the dinuclear vanadium–dinitrogen complexes produced only ammonia, while **1**, **2**, **3**, and **4** produced both ammonia and hydrazine [21,22]. The yields of NH<sub>3</sub> and N<sub>2</sub>H<sub>4</sub> were estimated from the peak intensities of NH<sub>4</sub><sup>+</sup> using <sup>1</sup>H NMR (7.04 ppm) and using the *p*-dimethylaminobenzaldehyde method using UV-vis spectra (458 nm), respectively (Figures S15 and S16). When using K[C<sub>10</sub>H<sub>8</sub>] as a reductant, the yields of NH<sub>3</sub> and N<sub>2</sub>H<sub>4</sub> were 47 and 11% for **1**, 38 and 16% for **2**, 78 and 7% for **3**, and 80 and 5% for **4** (per V atom), respectively (Tables 3 and S2). Their yields were higher than when using Na[C<sub>10</sub>H<sub>8</sub>]. Thus, the results suggest that the yield of products is dependent on the kind of alkali metal ions. The yield of NH<sub>3</sub> for **2** was less than that of **1**, and the yield of N<sub>2</sub>H<sub>4</sub> was higher than that of **1**. The result that the V–N<sub>N2</sub> bond length is longer in **2** than in **1** suggests that mononuclear vanadium species are more likely to form from the vanadium–dinitrogen complex because the steric repulsion of substituents is greater in **2** than in **1**. Therefore, the intermediates of the protonation reaction were estimated to be a hetero-dinuclear Na<sup>+</sup>/K<sup>+</sup>-V( $\mu$ -N<sub>2</sub>) complex, as in **4**. The yield with K[C<sub>10</sub>H<sub>8</sub>] as the reducing agent was higher than that with Na[C<sub>10</sub>H<sub>8</sub>], suggesting that potassium ions bound to N<sub>2</sub> ligands are more readily exchanged to protons than sodium ions. We have recently found and reported similar behavior in the triamidoamine–chromium–dinitrogen system [49].

**Table 3.** Quantification of ammonia and hydrazine produced from the reactions of 1–4 with reductants and proton sources [a].

Entry	Complex	Reductant	Proton Source	Yield [b] /%	
				NH <sub>3</sub> [c]	N <sub>2</sub> H <sub>4</sub> [c]
1	<b>1</b>	Na[C <sub>10</sub> H <sub>8</sub> ]	HOTf	8	0.4
2		K[C <sub>10</sub> H <sub>8</sub> ]		47	11
3	<b>2</b>	Na[C <sub>10</sub> H <sub>8</sub> ]	HOTf	5	11
4		K[C <sub>10</sub> H <sub>8</sub> ]		38	16
5	<b>3</b>	Na[C <sub>10</sub> H <sub>8</sub> ]	HOTf	7	n.d.
6		K[C <sub>10</sub> H <sub>8</sub> ]		77	7
7	<b>4</b>	K[C <sub>10</sub> H <sub>8</sub> ]	HOTf	80	5

[a] All reactions were carried out in THF at –78 °C under N<sub>2</sub>. [b] Yields are given for a vanadium ion, and these values are an average of three trials. [c] Yields of NH<sub>3</sub> and N<sub>2</sub>H<sub>4</sub> were determined by <sup>1</sup>H NMR measurement and *p*-dimethylaminobenzaldehyde method. Concentration: 6.7 × 10<sup>–3</sup> M for this work.



On the other hand, the yields of the protonation products of **3** and **4** were higher than those of **1** and **2**, and the yield of  $N_2H_4$  was less than one tenth of that of  $NH_3$ . This result suggests that protonation of mononuclear dinitrogen complexes gives higher yields of protonated products than dinuclear dinitrogen complexes and that the dicyclohexylmethyl groups in **3** or **4** surround the  $N_\alpha$  atom of the  $N_2$  ligand, protecting it from proton attack and preventing the formation of  $N_2H_4$  (Figure 5 right).

These findings suggest that the alkyl substituents on the secondary carbon atoms adjacent to the terminal N atom of triamidoamine stabilize the dimer structure, while the substituents on the tertiary carbon atoms destabilize the dimer structure or stabilize the monomer structure. These results also suggest that hetero-dinuclear dinitrogen complexes consisting of vanadium(II), alkali metal ions, and bridging  $N_2$  ligands are formed as intermediates in the protonation reactions of vanadium complexes **1**, **2**, and **3**. It was also found that hetero-dinuclear complexes produce both  $NH_3$  and  $N_2H_4$ , while the divanadium complexes produce only  $NH_3$ .

### 3. Materials and Methods

#### 3.1. General Procedures

All manipulations were carried out under an inert  $N_2$  or Ar atmosphere using either a vacuum and  $N_2$ /Ar gas manifold, or a MBraun MB 150B-G glovebox ( $N_2$ /Ar). Reagents and solvents employed were commercially available. All anhydrous solvents were purchased from Wako Ltd. and were bubbled with argon to degas. The ligand tris(2-isopropylaminoethyl)amine ( $H_3L^{iPr}$ ) was synthesized according to the literature methods [28].

#### 3.2. Physical Measurements

$^1H$ -,  $^{13}C$ -,  $^{15}N$ -, and  $^{51}V$ -NMR spectra were recorded on a JEOL JNM-ECA500, or a JNM-ECA600 FT NMR spectrometer operating at 500 MHz ( $^1H$ ), at 125.77 MHz ( $^{13}C$ ) in  $C_6D_6$  or  $DMSO-d_6$  at 298 K.  $^1H$  and  $^{13}C$  chemical shifts were referenced using residual protonated solvent resonance ( $C_6D_6$ : 7.16 ppm ( $^1H$ ) and 128.06 ppm ( $^{13}C$ ),  $DMSO-d_6$ : 2.50 ppm ( $^1H$ )).  $^{15}N$  and  $^{51}V$  NMR chemical shifts were externally referenced using  $HCONH_2$  (−266.712 ppm ( $^{15}N$ )) and  $VOCl_3$  (0.00 ppm ( $^{51}V$ )). Electronic absorption spectra were recorded on a JASCO V-770 spectrophotometer. FT-IR spectra were taken on an Agilent Cary 630 FTIR spectrophotometer. A resonance Raman spectroscopy was performed using a JASCO NRS-3300 spectrometer with 532 nm-wavelength Nd:YAG excitation source.

#### 3.3. X-ray Crystallography Procedures

The data for **1**, **2**, and **3** were measured on Rigaku R-Axis RAPID diffractometer using multi-layer mirror monochromated  $Mo K\alpha$  ( $\lambda = 0.71073 \text{ \AA}$ ) radiation. The data for **4** were measured on Rigaku R-Axis RAPID II diffractometer using multi-layer mirror monochromated  $Cu K\alpha$  ( $\lambda = 1.54178 \text{ \AA}$ ) radiation. Crystal data and experimental details are listed in Table S1. The calculations were performed with the Olex2 software package [50]. All structures were solved using ShelXT [51] structure solution program using the intrinsic phasing method, and the other atoms were found in subsequent Fourier maps. The structures were refined with ShelXL [52] using least squares minimization. All non-hydrogen atoms were anisotropically refined, unless otherwise stated. The hydrogen atoms were placed at their idealized positions, and the riding model was assumed, unless otherwise stated. CCDC-1970392 (**1**), 2167309 (**2**), 2167311 (**3**), 2167310 (**4**) contain the supplementary crystallographic data for this paper. These data can be obtained free of charge from The Cambridge Crystallographic Data Centre via [www.ccdc.cam.ac.uk/data\\_request/cif](http://www.ccdc.cam.ac.uk/data_request/cif), accessed on 22 August 2022.

#### 3.4. Synthesis of Tris(2-(3-pentylamino)ethyl)amine ( $H_3L^{Pen}$ )

Tris(2-aminoethyl)amine (14.6 g, 0.10 mol) was added to excess 3-pentanone (100 mL) and refluxed with a Dean–Stark trap overnight. The excess 3-pentanone was removed by evaporation. The mixture was cooled to 0 °C, and MeOH (50.0 mL) was added. Sodium

borohydride (11.7 g, 0.31 mol) was added, and the mixture was stirred overnight at R.T. Sodium hydroxide (12.3 g, 0.31 mol) in water (100 mL) was added, and the aqueous layer was extracted 3 times by Et<sub>2</sub>O (100 mL). The organic layer was dried over Na<sub>2</sub>SO<sub>4</sub>, and the solvent was removed by evaporation. The mixture was distilled to give a light-yellow oil (yield 33.1 g, 93%). <sup>1</sup>H NMR (500 MHz, C<sub>6</sub>D<sub>6</sub>, 298 K): δ (ppm) 0.950 (t, 18H, -CH<sub>3</sub>), 1.45 (quin, 12H, CH-CH<sub>2</sub>-CH<sub>3</sub>), 2.37 (quin, 3H, CH-(CH<sub>2</sub>CH<sub>3</sub>)<sub>2</sub>), 2.50 (t, 6H, NH-CH<sub>2</sub>-CH<sub>2</sub>), 2.62 (t, 6H, NH-CH<sub>2</sub>-CH<sub>2</sub>). <sup>13</sup>C{<sup>1</sup>H} NMR (125.77 MHz, C<sub>6</sub>D<sub>6</sub>, 298 K): δ (ppm) 10.18, 26.53, 45.34, 55.13, 60.64.

### 3.5. Synthesis of Tris(2-dicyclohexylmethylaminoethyl)amine (H<sub>3</sub>L<sup>Cy2</sup>)

Tris(2-aminoethyl)amine (14.6 g, 0.10 mol) was added to dicyclohexyl ketone (77.6 g, 0.40 mol) in toluene (100 mL) and refluxed with a Dean–Stark trap for 2 days. The excess dicyclohexyl ketone was removed in vacuo. The mixture was cooled to 0 °C, and MeOH (50.0 mL) was added. Sodium borohydride (11.7 g, 0.31 mol) was added, and the mixture was stirred overnight at R.T. Sodium hydroxide (12.3 g, 0.31 mol) in water (100 mL) was added, and the aqueous layer was extracted 3 times by Et<sub>2</sub>O (100 mL). The organic layer was dried over Na<sub>2</sub>SO<sub>4</sub>, and the solvent was removed by evaporation. The mixture MeOH (100 mL) and hexane (10 mL) was added and stored at -30 °C. The white solid was filtered and washed using solvent (2-propanol:hexane = 10:1). The white solid was resolved using CHCl<sub>3</sub>. Recrystallization was done by standing still in R.T. and white crystals were obtained (yield 43.5 g, 64%). <sup>1</sup>H NMR (500 MHz, C<sub>6</sub>D<sub>6</sub>, 298 K): δ (ppm) 1.12–2.02 (m, 69H, Cy<sub>2</sub>-CH-), 2.62 (t, 6H, NH-CH<sub>2</sub>-CH<sub>2</sub>), 2.82 (t, 6H, NH-CH<sub>2</sub>-CH<sub>2</sub>). <sup>13</sup>C{<sup>1</sup>H} NMR (125.77 MHz, C<sub>6</sub>D<sub>6</sub>, 298 K): δ (ppm) 27.23, 27.32, 27.38, 29.11, 31.81, 41.42, 50.68, 56.46, 68.90.

### 3.6. Synthesis of [[V(L<sup>iPr</sup>)<sub>2</sub>(μ-<sup>14</sup>N<sub>2</sub>)] (1)

A 20 mL Schlenk flask was charged with H<sub>3</sub>L<sup>iPr</sup> (1.0 g, 3.7 mmol) and diethyl ether (4.00 mL) and cooled to -78 °C under nitrogen (<sup>14</sup>N<sub>2</sub>). *n*-butyllithium (4.2 mL, 11.0 mmol, 2.6 M in hexane) was added using a syringe. After 15 min, the reaction mixture was slowly warmed to 25 °C and was stirred for 1 h at room temperature. The reaction mixture was then cooled to -78 °C and VCl<sub>3</sub>THF<sub>3</sub> (1.4 g, 3.7 mmol) was added via cannula to another Schlenk flask. The reaction mixture was again slowly warmed to 25 °C and was stirred overnight. The solvent was removed in vacuo, and the residue was extracted with diethyl ether (6 mL). The extract was filtered through Celite. The diethyl ether extract was transferred to a 20 mL Schlenk flask and stored in a fridge at -35 °C. [[VL<sup>iPr</sup>]<sub>2</sub>(μ-N<sub>2</sub>)] was obtained as dark green crystals (yield 0.57 g, 46%). <sup>1</sup>H NMR (500 MHz, C<sub>6</sub>D<sub>6</sub>, 298 K): δ (ppm) 1.44 (d, 36H, -CH<sub>3</sub>), 2.40 (t, 12H, NH-CH<sub>2</sub>-CH<sub>2</sub>), 3.29 (t, 12H, N-CH<sub>2</sub>-CH<sub>2</sub>), 5.27 (sep, 6H, CH-(CH<sub>3</sub>)<sub>2</sub>), <sup>13</sup>C{<sup>1</sup>H} NMR (125.77 MHz, C<sub>6</sub>D<sub>6</sub>, 298 K): δ (ppm) 23.46, 48.22, 53.11, 60.84, <sup>51</sup>V NMR (131.56 MHz, C<sub>6</sub>D<sub>6</sub>, 298 K): δ (ppm) -211.1. FT IR (ATR, cm<sup>-1</sup>): 2957, 2916, 2892, 2851, 2788, 2652, 1457, 1438, 1380, 1364, 1347, 1332, 1328, 1282, 1259, 1239, 1202, 1155, 1129, 1099, 1077, 1056, 1028, 1002, 967, 939, 905, 862, 840, 818, 796, 789, 747, 618, 592, 572, 549, 495, 469.

### 3.7. [[V(L<sup>iPr</sup>)<sub>2</sub>(μ-<sup>15</sup>N<sub>2</sub>)] (1')

Complex 1' was synthesized using the same method as complex 1 using <sup>15</sup>N<sub>2</sub> instead of <sup>14</sup>N<sub>2</sub>. Complex 1' was obtained as dark green crystals (yield 0.29 g, 24%). <sup>15</sup>N-NMR (60.815 MHz, C<sub>6</sub>D<sub>6</sub>, 298 K): δ (ppm) 25.22. FT-IR (KBr, cm<sup>-1</sup>): 779 (ν(V-<sup>15</sup>N)).

### 3.8. Synthesis of [[V(L<sup>Pen</sup>)<sub>2</sub>(μ-<sup>14</sup>N<sub>2</sub>)] (2)

Complex 2 was synthesized using the same method as complex 1 using H<sub>3</sub>L<sup>Pen</sup> instead of H<sub>3</sub>L<sup>iPr</sup>. Complex 2 was obtained as purple crystals (yield 1.1 g, 89%). <sup>1</sup>H NMR (500 MHz, C<sub>6</sub>D<sub>6</sub>, 298 K): δ (ppm) 1.15 (t, 36H, -CH<sub>3</sub>), 1.74 (quin, 24H, CH-CH<sub>2</sub>-CH<sub>3</sub>), 2.37 (t, 12H, N-CH<sub>2</sub>-CH<sub>2</sub>), 3.20 (t, 6H, N-CH<sub>2</sub>-CH<sub>2</sub>), 4.77 (quin, 6H, CH-(CH<sub>2</sub>CH<sub>3</sub>)<sub>2</sub>). <sup>13</sup>C{<sup>1</sup>H} NMR (125.77 MHz, C<sub>6</sub>D<sub>6</sub>, 298 K): δ (ppm) 12.51, 27.71, 48.57, 53.05, 71.52. <sup>51</sup>V NMR (131.56 MHz, C<sub>6</sub>D<sub>6</sub>, 298 K): δ (ppm) -47.55. FT IR (ATR, cm<sup>-1</sup>): 2955, 2920, 2892, 2870, 2845, 2788, 1444,

1371, 1341, 1330, 1280, 1259, 1237, 1205, 1144, 1127, 1107, 1047, 1026, 993, 952, 905, 898, 866, 857, 834, 827, 812, 758, 728, 663, 642, 590, 559, 549, 572, 549, 527, 519, 486.

### 3.9. Synthesis of $[(V(L^{Pen}))_2(\mu^{-15}N_2)]$ (**2'**)

Complex **2'** was synthesized using the same method as complex **2** using  $^{15}N_2$  instead of  $^{14}N_2$ . Complex **2'** was obtained as purple crystals (yield 0.49 g, 41%).  $^{15}N$  NMR (60.815 MHz,  $C_6D_6$ , 298 K):  $\delta$  (ppm) 41.59. FT IR (ATR,  $cm^{-1}$ ): 715 ( $\nu(V^{-15}N)$ ).

### 3.10. Synthesis of $[V(L^{Cy2})]$ (**3**)

The complex **3** was synthesized using the same method as complex **1** using  $H_3L^{Cy2}$  in place of  $H_3L^{iPr}$ . THF for reaction solvent and hexane for recrystallization were used instead of diethyl ether (yield 0.79 g, 74%). FT IR (ATR,  $cm^{-1}$ ): 2955, 2920, 2892, 2870, 2845, 2788, 1444, 1371, 1341, 1330, 1280, 1259, 1237, 1205, 1144, 1127, 1107, 1047, 1026, 993, 952, 905, 898, 866, 857, 834, 827, 812, 758, 728, 663, 642, 590, 559, 549, 572, 549, 527, 519, 486.

### 3.11. Synthesis of $[VK(L^{Cy2})(\mu^{-14}N_2)(18-crown-6)]$ (**4**)

A 15 mL vial was inserted with complex **3** (0.20 g, 0.27 mmol) and THF (6 mL) under nitrogen gas. A quantity of K metals (0.11 g, 2.7 mmol, 10 eq.) was added to the solution, and the solution was stirred at R.T. overnight. The mixture was filtered through Celite, and the filtrate was added 18-crown-6-ether (79.8 mg, 0.30 mmol) in THF (1 mL). The mixture was stirred at R.T. for 1 min. Hexane (6 mL) was slowly added to the reaction mixture. Recrystallization of the complex **4** at  $-35$  °C yielded a green crystal (0.13 mg, 39%). FT IR (ATR,  $cm^{-1}$ ): 1830, 1818 ( $\nu(^{14}N-^{14}N)$ ).

### 3.12. Synthesis of $[VK(L^{Cy2})(\mu^{-15}N_2)(18-crown-6)]$ (**4'**)

Complex **4'** was synthesized using the same method as complex **4** using  $^{15}N_2$  instead of  $^{14}N_2$ . Complex **4'** was obtained as green crystals (60.2 mg, 18%). FT IR (ATR,  $cm^{-1}$ ): 1768, 1759 ( $\nu(^{15}N-^{15}N)$ ).

### 3.13. Protonation of **1**, **2**, **3**, and **4** with Reductant and Proton Source

A 6 mL THF solution of the reductant ( $[M[C_{10}H_8]]$  ( $M = Na, K$ )), freshly prepared from alkali metal (1.1 mmol, 80 eq.) and naphthalene (0.15 mg, 1.1 mmol, 80 eq.) in a thick-walled glass bomb, was added to a 5 mL THF solution of **1** (10.0 mg,  $1.5 \times 10^{-2}$  mmol) at  $-78$  °C, and the mixture was stirred for 1 h under  $N_2$ . The reaction mixture turned from deep green to greenish brown. HOTf (0.17 g, 1.1 mmol) was added to the vigorously stirred reaction mixture of **1**, and the resultant solution was slowly warmed to 25 °C. After the solution was stirred for 1 h at room temperature, the solvents were removed under reduced pressure to give a white solid containing ammonium and hydrazinium salts. The residue in the Schlenk tube was washed using diethyl ether and then, extracted using  $H_2O$  (10 mL), and solvents of an aliquot (5 mL) of this solution were evaporated. The residue was analyzed using  $^1H$  NMR methods (for  $NH_3$ ). The other aliquot reacted with *p*-dimethylaminobenzaldehyde (for  $N_2H_4$ ).

### 3.14. $NH_3$ Quantification Procedure

Quantification of ammonium salts was estimated using  $^1H$  NMR spectroscopy. The quantification of  $NH_4^+$  was carried out using the method reported by Ashley and co-workers [53].  $^{14}NH_4^+$  was integrated relative to the vinylic protons of 2,5-dimethylfuran, contained within a  $DMSO-d_6$  capillary insert ( $\delta$ :5.83, s, 2H), which was calibrated using a standard  $5.2 \times 10^{-2}$  M solution of  $NH_4^+$  in  $DMSO-d_6$  (Figure S15 and Table S2).

### 3.15. $N_2H_4$ Quantification Procedure

The quantification of  $N_2H_5^+$  was carried out using the method reported by Ashley and co-workers [53]. The aliquots were analyzed for  $N_2H_4$  via UV-vis spectroscopy using a standard spectrophotometric method, which reacted with an acidic *p*-dimethylaminobenzaldehyde

solution and generated a yellow azine dye with a characteristic electronic absorption feature at 458 nm. The  $\text{N}_2\text{H}_4$  in aliquot was quantified by comparison to the calibration curve (Figure S16).

#### 4. Conclusions

In this study, we prepared vanadium(III) complexes with newly designed triamidoamine ligands ( $[\text{L}^{\text{R}}]^{3-}$  R = iPr, Pen, and Cy<sub>2</sub>) (**1**, **2**, and **3**, respectively) under  $\text{N}_2$ , which have tertiary C atoms adjacent to the terminal N atoms of the ligand. The X-ray structure analyses for **1**, **2**, and **3** revealed that complexes **1** and **2** were divanadium–dinitrogen complexes with a  $\mu\text{-N}_2$  ligand between two vanadium ions in the end-on mode ( $[\{\text{V}(\text{L}^{\text{R}})\}_2(\text{N}_2)]$  R = iPr and Pen), while complex **3** was a mononuclear vanadium complex without  $\text{N}_2$  coordination,  $[\text{V}(\text{L}^{\text{Cy}_2})]$ . These results indicate that complexes **1** and **2** with isopropyl and pentyl groups, respectively, can form dimeric structures, but due to steric repulsion between the dicyclohexylmethyl groups of the ligands, such a dimeric structure was not formed in complex **3**. The evidence of this is that all V–N<sub>amido</sub> bond lengths around the vanadium(III) ion are the longest among complex **2** and the divanadium(III)–dinitrogen complexes with triamidoamine ligands reported so far. Furthermore, complex **3**, which has an even larger dicyclohexylmethyl group, did not form a dimer structure due to steric repulsion of the dicyclohexylmethyl group and formed a mononuclear complex. Reduction in complex **3** with potassium metal in the presence of 18-crown-6-ether produced the thermally unstable vanadium(II)–dinitrogen complex (**4**). The crystal structure of **4** was revealed to be a hetero-dinuclear complex with a bridging  $\text{N}_2$  ligand between V(II) and the  $\text{K}^+$  ion surrounded with 18-crown-6-ether.

Reactions of complexes **1**, **2**, **3**, and **4** with  $\text{M}[\text{C}_{10}\text{H}_8]$  (M =  $\text{Na}^+$  or  $\text{K}^+$ ) and HOTf yielded  $\text{NH}_3$  and  $\text{N}_2\text{H}_4$ , which are significantly different from our previous results using divanadium–dinitrogen complexes with similar triamidoamine ligands that we reported as releasing only ammonia [21,22]. This may be explained due to the following facts. In the case of the previously reported divanadium–dinitrogen complexes with a secondary C atom on the terminal N atom of the triamidoamine ligand, the addition of alkali metal ions resulted in the formation of a divanadium–dinitrogen complex as a reaction intermediate. On the other hand, in the cases of **1**, **2**, **3**, and **4** with tertiary C atoms instead of secondary C atoms, the addition of alkali metal ions resulted in the formation of a hetero-dinuclear nitrogen complex. Surrounding the  $\text{N}_\alpha$  atom with large substituents increases the yield of  $\text{NH}_3$  and conversely, decreases the yield of  $\text{N}_2\text{H}_4$ . These results indicate that the large steric repulsion around the  $\text{N}_\alpha$  atom prevents the protonation reaction into the  $\text{N}_\alpha$  atom.

Here, we have found that changing the carbon atom adjacent to the terminal N atom of a triamidoamine ligand from a secondary carbon to a tertiary carbon can have a significant effect on structure and reactivity. These results provide an important finding to dinitrogen fixation catalysis and the model study of nitrogenase.

**Supplementary Materials:** The following supporting information can be downloaded at: <https://www.mdpi.com/article/10.3390/molecules27185864/s1>, Figure S1: Raman spectra of **1**; Figure S2: Raman spectra of **2**; Figure S3: IR spectra of **1**; Figure S4: IR spectra of **2**; Figure S5: IR spectra of **4**; Figure S6:  $^1\text{H}$  NMR spectrum of **1**; Figure S7:  $^1\text{H}$  NMR spectrum of **2**; Figure S8:  $^{15}\text{N}$  NMR spectrum of **1'**; Figure S9:  $^{15}\text{N}$  NMR spectrum of **2'**; Figure S10:  $^{51}\text{V}$  NMR spectrum of **1**; Figure S11:  $^{51}\text{V}$  NMR spectrum of **2**; Figure S12:  $^1\text{H}$  NMR spectra of **3**; Figure S13:  $^1\text{H}$  NMR spectrum of **4**; Figure S14:  $^1\text{H}$  NMR spectra of  $\text{H}_3\text{L}^{\text{Cy}_2}$  and **4**; Figure S15:  $^1\text{H}$  NMR spectrum of  $^{14}\text{NH}_4^+$ ; Figure S16: Calibration curves for hydrazine quantification; Table S1: Experimental Data for X-ray Diffraction studies on Crystalline Complexes **1**, **2**, **3**, and **4**; Table S2: Yields of  $\text{NH}_3$  and  $\text{N}_2\text{H}_4$ . The CCDC deposition numbers 1970392 (**1**), 2167309 (**2**), 2167311 (**3**), and 2167310 (**4**) contain the supplementary crystallographic data for this paper, which can be obtained free of charge via emailing [data\\_request@ccdc.cam.ac.uk](mailto:data_request@ccdc.cam.ac.uk), or by contacting The Cambridge Crystallographic Data Centre at 12 Union Road, Cambridge CB2 1EZ, UK; Fax: +44-1223-336033.

**Author Contributions:** Conceptualization, Y.K. (Yoshiaki Kokubo) and Y.K. (Yuji Kajita); methodology, Y.K. (Yoshiaki Kokubo) and Y.K. (Yuji Kajita); validation, Y.K. (Yoshiaki Kokubo) and Y.K. (Yuji Kajita); formal analysis, Y.K. (Yoshiaki Kokubo), Y.K. (Yuji Kajita), I.I., K.N., W.H. and T.O.; investigation, Y.K. (Yoshiaki Kokubo) and Y.K. (Yuji Kajita); data curation, Y.K. (Yoshiaki Kokubo); writing—original draft preparation, Y.K. (Yoshiaki Kokubo) and Y.K. (Yuji Kajita); writing—review and editing, Y.K. (Yuji Kajita), S.K. and H.M.; supervision, Y.K. (Yuji Kajita), S.K. and H.M.; project administration, Y.K. (Yuji Kajita); funding acquisition, Y.K. (Yuji Kajita) and H.M. All authors have read and agreed to the published version of the manuscript.

**Funding:** This research was funded by the Japan Society for the Promotion of Science (JSPS), grant number (B) 20H027520 and (C) 20K05545.

**Institutional Review Board Statement:** Not applicable.

**Informed Consent Statement:** Not applicable.

**Data Availability Statement:** The data presented in this study are contained within this article and are supported by the data in the Supplementary Materials.

**Acknowledgments:** We thank Haruyo Nagao (Institute for Molecular Science) for  $^{15}\text{N}$  NMR spectroscopy measurement. This work was supported by the Nanotechnology Platform Program (Institute for Molecular Science) (JPMXP09S21MS1012) and the Advanced Research Infrastructure for Materials and Nanotechnology (JPMXP1222MS1018) of the Ministry of Education, Culture, Sports, Science and Technology (MEXT), Japan. We also acknowledge the Japan Society for the Promotion of Science (JSPS) for a grant in aid of scientific research (B and C) (20H027520, 20K05545).

**Conflicts of Interest:** The authors declare no conflict of interest.

**Sample Availability:** Samples are not available from the corresponding authors.

## References

1. Hales, B.J.; Case, E.E.; Morningstar, J.E.; Dzeda, M.F.; Mauterer, L.A. Isolation of a New Vanadium-Containing Nitrogenase from *Azotobacter vinelandii*. *Biochemistry* **1986**, *25*, 7251–7255. [[CrossRef](#)] [[PubMed](#)]
2. Arber, J.M.; Dobson, B.R.; Eady, R.R.; Stevens, P.; Hasnain, S.S.; Garner, C.D.; Smith, B.E. Vanadium K-edge X-ray absorption spectrum of the VFe protein of the vanadium nitrogenase of *Azotobacter chroococcum*. *Nature* **1986**, *325*, 372–374. [[CrossRef](#)]
3. Eady, R.R. Structure-Function Relationships of Alternative Nitrogenases. *Chem. Rev.* **1996**, *96*, 3013–3030. [[CrossRef](#)]
4. Rehder, D. The coordination chemistry of vanadium as related to its biological functions. *Coord. Chem. Rev.* **1999**, *182*, 297–322. [[CrossRef](#)]
5. Smith, B.E. Structure, function, and biosynthesis of the metallosulfur clusters in nitrogenases. *Adv. Inorg. Chem.* **1999**, *47*, 159–218.
6. Eady, R.R. Current status of structure function relationships of vanadium nitrogenase. *Coord. Chem. Rev.* **2003**, *237*, 23–30. [[CrossRef](#)]
7. Janas, Z.; Sobota, P. Aryloxo and thiolato vanadium complexes as chemical models of the active site of vanadium nitrogenase. *Coord. Chem. Rev.* **2005**, *249*, 2144–2155. [[CrossRef](#)]
8. Sippel, D.; Einsle, O. The structure of vanadium nitrogenase reveals an unusual bridging ligand. *Nat. Chem. Biol.* **2017**, *13*, 956–960. [[CrossRef](#)]
9. Sippel, D.; Rohde, M.; Netzer, J.; Trncik, C.; Gies, J.; Grunau, K.; Djurdjevic, I.; Decamps, L.; Einsle, O. A bound reaction intermediate sheds light on the mechanism of nitrogenase. *Science* **2018**, *359*, 1484–1489. [[CrossRef](#)]
10. Duman, L.M.; Sita, L.R. Group 5 Transition Metal-Dinitrogen Complexes. In *Transition Metal-Dinitrogen Complexes*, 1st ed.; Nishibayashi, Y., Ed.; Wiley-VCH Verlag GmbH & Co. KGaA: Weinheim, Germany, 2019; pp. 159–220.
11. Rehder, D.; Woitha, C.; Priebsch, W.; Gailus, H. Trans-[Na(thf)][V(N<sub>2</sub>)<sub>2</sub>(Ph<sub>2</sub>PCH<sub>2</sub>CH<sub>2</sub>PPh<sub>2</sub>)<sub>2</sub>]: Structural characterization of a dinitrogenvanadium complex, a functional model for vanadiumnitrogenase. *J. Chem. Soc. Chem. Commun.* **1992**, *28*, 364–365. [[CrossRef](#)]
12. Woitha, C.; Rehder, D. Vanadium(-I) Dinitrogen Complexes with N<sub>2</sub> Coordinated End-on: Functional Models for the “Alternative Nitrogenase”. *Angew. Chem. Int. Ed. Engl.* **1990**, *29*, 1438–1440. [[CrossRef](#)]
13. Gailus, H.; Woitha, C.; Rehder, D. Dinitrogenvanadates(-I): Synthesis, reactions and conditions for their stability. *J. Chem. Soc. Dalton Trans.* **1994**, *23*, 3471–3477. [[CrossRef](#)]
14. Smythe, N.C.; Schrock, R.R.; Müller, P.; Weare, W.W. Synthesis of [(HIPTNCH<sub>2</sub>CH<sub>2</sub>)<sub>3</sub>N]V Compounds (HIPT) 3,5-(2,4,6-i-Pr<sub>3</sub>C<sub>6</sub>H<sub>2</sub>)<sub>2</sub>C<sub>6</sub>H<sub>3</sub>) and an Evaluation of Vanadium for the Reduction of Dinitrogen to Ammonia. *Inorg. Chem.* **2006**, *45*, 9197–9205. [[CrossRef](#)] [[PubMed](#)]
15. Nishibayashi, Y.; Tanabe, Y. Recent advances in nitrogen fixation upon vanadium complexes. *Coord. Chem. Rev.* **2019**, *381*, 135–150.



16. Ferguson, R.; Solari, E.; Floriani, C.; Chiesi-Villa, A.; Rizzoli, C. Fixation and Reduction of Dinitrogen by Vanadium(II) and Vanadium(III): Synthesis and Structure of Dinitrogenmesitylvanadium Complexes. *Angew. Chem. Int. Ed. Engl.* **1993**, *32*, 396–397. [[CrossRef](#)]
17. Ferguson, R.; Solari, E.; Floriani, C.; Osella, D.; Ravera, M.; Re, N.; Chiesi-Villa, A.; Rizzoli, C. Stepwise reduction of dinitrogen occurring on a divanadium model compound: A synthetic, structural, magnetic, electrochemical, and theoretical investigation on the  $[V=N=N=N](n+)$  [ $n = 4-6$ ] based complexes. *J. Am. Chem. Soc.* **1997**, *119*, 10104–10115. [[CrossRef](#)]
18. Liu, G.; Liang, X.; Meetsma, A.; Hessen, B. Synthesis and structure of an aminoethyl-functionalized cyclopentadienyl vanadium(i) dinitrogen complex. *Dalton Trans.* **2010**, *39*, 7891–7893. [[CrossRef](#)]
19. Vidyaratne, I.; Crewdson, P.; Lefebvre, E.; Gambarotta, S. Dinitrogen Coordination and Cleavage Promoted by a Vanadium Complex of a  $\sigma,\pi,\sigma$ -Donor Ligand. *Inorg. Chem.* **2007**, *46*, 8836–8842. [[CrossRef](#)]
20. Sekiguchi, Y.; Arashiba, K.; Tanaka, H.; Eizawa, A.; Nakajima, K.; Yoshizawa, K.; Nishibayashi, Y. Catalytic Reduction of Molecular Dinitrogen to Ammonia and Hydrazine Using Vanadium Complexes. *Angew. Chem. Int. Ed.* **2018**, *57*, 9064–9068. [[CrossRef](#)]
21. Kokubo, Y.; Yamamoto, C.; Tsuzuki, K.; Nagai, T.; Katayama, A.; Ohta, T.; Ogura, T.; Wasada-Tsutsui, Y.; Kugimiya, S.; Masuda, H. Dinitrogen Fixation by Vanadium Complexes with a Triamidoamine Ligand. *Inorg. Chem.* **2018**, *57*, 11884–11894. [[CrossRef](#)]
22. Kokubo, Y.; Wasada-Tsutsui, Y.; Yomura, S.; Yanagisawa, S.; Kubo, M.; Kugimiya, S.; Kajita, Y.; Ozawa, T.; Masuda, H. Syntheses, Characterizations, and Crystal Structures of Dinitrogen-Divanadium Complexes Bearing Triamidoamine Ligands. *Eur. J. Inorg. Chem.* **2020**, *2020*, 1456–1464. [[CrossRef](#)]
23. Schrock, R.R. Transition Metal Complexes That Contain a Triamidoamine Ligand. *Acc. Chem. Res.* **1997**, *30*, 9–16. [[CrossRef](#)]
24. Cummins, C.C.; Lee, J.; Schrock, R.R.; Davis, W.M. Trigonalmonopyramidal M(III) complexes of the type  $M(N_3N)$  [ $M =$  titanium, vanadium, chromium, manganese, iron;  $N_3N = [(tert-BuMe_2Si)NCH_2CH_2]_3N$ ]. *Angew. Chem. Int. Ed. Engl.* **1992**, *31*, 1501–1503. [[CrossRef](#)]
25. Cummins, C.C.; Lee, J.; Schrock, R.R. Phosphinidenetantalum(V) complexes  $[(N_3N)Ta = PR]$  as phospho-Wittig reagents ( $R = Ph, Cy, tert-Bu$ ;  $N_3N = (Me_3SiNCH_2CH_2)_3N$ ). *Angew. Chem. Int. Ed. Engl.* **1993**, *32*, 756–759. [[CrossRef](#)]
26. Cummins, C.C.; Schrock, R.R. Synthesis of an iron(IV) cyanide complex that contains the triamidoamine ligand  $[(tert-BuMe_2SiNCH_2CH_2)_3N]_3^-$ . *Inorg. Chem.* **1994**, *33*, 395–396. [[CrossRef](#)]
27. Cummins, C.C.; Schrock, R.R.; Davis, W.M. Synthesis of Terminal Vanadium(V) Imido, Oxo, Sulfido, Selenido, and Tellurido Complexes by Imido Group or Chalcogen Atom Transfer to Trigonal Monopyramidal  $V[N_3N]$  ( $N_3N = [(Me_3SiNCH_2CH_2)_3N]_3^-$ ). *Inorg. Chem.* **1994**, *33*, 1448–1457. [[CrossRef](#)]
28. Duan, Z.; Verkade, J.G. Synthesis and Characterization of a Novel Azatitanatranne. *Inorg. Chem.* **1995**, *34*, 4311–4316. [[CrossRef](#)]
29. Naiini, A.A.; Menge, W.M.P.B.; Verkade, J.G. Titanatranes and azatitanatranes: Nucleophilic substitution reactions on the axial position. *Inorg. Chem.* **1991**, *30*, 5009–5012. [[CrossRef](#)]
30. Nomura, K.; Schrock, R.R.; Davis, W.M. Synthesis of Vanadium(III), -(IV), and -(V) Complexes That Contain the Pentafluorophenyl-Substituted Triamidoamine Ligand  $[(C_6F_5NCH_2CH_2)_3N]_3^-$ . *Inorg. Chem.* **1996**, *35*, 3695–3701. [[CrossRef](#)]
31. Freundlich, J.S.; Schrock, R.R. Synthesis of Triamidoamine Complexes of Niobium. *Inorg. Chem.* **1996**, *35*, 7459–7461. [[CrossRef](#)]
32. Rosenberger, C.; Schrock, R.R.; Davis, W.M. Synthesis and Structure of a Trigonal Monopyramidal Vanadium(III) Complex,  $[(C_6F_5NCH_2)_3N]V$ , and the Vanadium(IV) Product of Its Oxidation,  $\{[(C_6F_5NCH_2)_2N(CH_2CH_2NHC_6F_5)]V(O)\}_2$ . *Inorg. Chem.* **1997**, *36*, 123–125. [[CrossRef](#)]
33. Pinkas, J.; Gaul, B.; Verkade, J.G. Group 13 azatranes: Synthetic, conformational, and configurational features. *J. Am. Chem. Soc.* **1993**, *115*, 3925–3931. [[CrossRef](#)]
34. Plass, W.; Verkade, J.G. A novel transmetalation reaction: A route to transition metallatranes. *J. Am. Chem. Soc.* **1992**, *114*, 2275–2276. [[CrossRef](#)]
35. Cummins, C.C.; Schrock, R.R.; Davis, W.M. Synthesis of Vanadium and Titanium Complexes of the Type  $RM[(Me_3SiNCH_2CH_2)_3N]$  ( $R = Cl, Alkyl$ ) and the Structure of  $ClV[(Me_3SiNCH_2CH_2)_3N]$ . *Organometallics* **1992**, *11*, 1452–1454. [[CrossRef](#)]
36. Christou, V.; Arnold, J. Synthesis of monomeric terminal chalcogenides via template-induced disilylchalcogenide elimination: Structure of  $[ETa-\{Me_3SiNCH_2CH_2\}_3N]$  ( $E =$  selenium, tellurium). *Angew. Chem. Int. Ed. Engl.* **1993**, *32*, 1450–1452. [[CrossRef](#)]
37. Yandulov, D.V.; Schrock, R.R.; Rheingold, A.L.; Ceccarelli, C.; Davis, W.M. Synthesis and Reactions of Molybdenum Triamidoamine Complexes Containing Hexaisopropylterphenyl Substituents. *Inorg. Chem.* **2003**, *42*, 796–813. [[CrossRef](#)]
38. Yandulov, D.V.; Schrock, R.R. Catalytic Reduction of Dinitrogen to Ammonia at a Single Molybdenum Center. *Science* **2003**, *301*, 76–78. [[CrossRef](#)]
39. Yandulov, D.V.; Schrock, R.R. Studies Relevant to Catalytic Reduction of Dinitrogen to Ammonia by Molybdenum Triamidoamine Complexes. *Inorg. Chem.* **2005**, *44*, 1103–1117. [[CrossRef](#)]
40. Smythe, N.C.; Schrock, R.R.; Müller, P.; Weare, W.W. Synthesis of  $[(HIPTNCH_2CH_2)_3N]Cr$  Compounds ( $HIPT = 3,5-(2,4,6-i-Pr_3C_6H_2)_2C_6H_3$ ) and an Evaluation of Chromium for the Reduction of Dinitrogen to Ammonia. *Inorg. Chem.* **2006**, *45*, 7111–7118. [[CrossRef](#)]
41. Doyle, L.R.; Woolees, A.J.; Liddle, S.T. Liddle Bimetallic Cooperative Cleavage of Dinitrogen to Nitride and Tandem Frustrated Lewis Pair Hydrogenation to Ammonia. *Angew. Chem. Int. Ed.* **2019**, *58*, 6674–6677. [[CrossRef](#)]
42. Ghana, P.; van Krüchten, F.D.; Spaniol, T.P.; van Leusen, J.; Kögerler, P.; Okuda, J. Conversion of dinitrogen to tris(trimethylsilyl)amine catalyzed by titanium triamido-amine complexes. *Chem. Commun.* **2019**, *55*, 3231–3234. [[CrossRef](#)] [[PubMed](#)]

43. Doyle, L.R.; Wooles, A.J.; Jenkins, L.C.; Tuna, F.; McInnes, E.J.L.; Liddle, S.T. Catalytic Dinitrogen Reduction to Ammonia at a Triamidoamine–Titanium Complex. *Angew. Chem. Int. Ed.* **2018**, *57*, 6314–6318. [[CrossRef](#)] [[PubMed](#)]
44. Shih, K.-Y.; Schrock, R.R.; Kempe, R. Synthesis of Molybdenum Complexes That Contain Silylated Triamidoamine Ligands. A *p*-Dinitrogen Complex, Methyl and Acetylide Complexes, and Coupling of Acetylides. *J. Am. Chem. Soc.* **1994**, *116*, 8804–8805. [[CrossRef](#)]
45. Addison, A.W.; Rao, T.N.; Reedijk, J.; van Rijn, J.; Verschoor, G.C. Synthesis, structure, and spectroscopic properties of copper(II) compounds containing nitrogen–sulphur donor ligands; the crystal and molecular structure of aqua [1,7-bis(N-methylbenzimidazol-2'-yl)-2,6-dithiaheptane]copper(II) perchlorate. *J. Chem. Soc. Dalton Trans.* **1984**, *7*, 1349–1356. [[CrossRef](#)]
46. Singh, D.; Buratto, W.R.; Torres, J.F.; Murray, L.J. Activation of Dinitrogen by Polynuclear Metal Complexes. *Chem. Rev.* **2020**, *120*, 5517–5581. [[CrossRef](#)]
47. Evans, D.F. The determination of the paramagnetic susceptibility of substances in solution by nuclear magnetic resonance. *J. Chem. Soc.* **1959**, 2003–2005. [[CrossRef](#)]
48. Sur, S.K. Measurement of magnetic susceptibility and magnetic moment of paramagnetic molecules in solution by high-field Fourier transform NMR spectroscopy. *J. Magn. Reson.* **1989**, *82*, 169–173. [[CrossRef](#)]
49. Kokubo, Y.; Tsuzuki, K.; Sugiura, H.; Yomura, S.; Wasada-Tsutsui, Y.; Ozawa, T.; Yanagisawa, S.; Kubi, M.; Kugmiya, S.; Masuda, H.; et al. Syntheses, Characterizations, Crystal Structures, and Protonation Reactions of Dinitrogen Chromium Complexes Supported with Triamidoamine Ligands. *Inorg. Chem.* **2022**, submitted for publication.
50. Dolomanov, O.V.; Bourhis, L.J.; Gildea, R.J.; Howard, J.A.K.; Puschmann, H. OLEX2: A complete structure solution, refinement and analysis program. *J. Appl. Crystallogr.* **2009**, *42*, 339–341. [[CrossRef](#)]
51. Sheldrick, G.M. SHELXT—Integrated space-group and crystal-structure determination. *Acta Crystallogr. Sect. A Found. Adv.* **2015**, *71*, 3–8. [[CrossRef](#)]
52. Sheldrick, G.M. A short history of SHELX. *Acta Crystallogr. Sect. A Found. Crystallogr.* **2008**, *64*, 112–122. [[CrossRef](#)] [[PubMed](#)]
53. Hill, P.J.; Doyle, L.R.; Crawford, A.D.; Myers, W.K.; Ashley, A.E. Selective Catalytic Reduction of N<sub>2</sub> to N<sub>2</sub>H<sub>4</sub> by a Simple Fe Complex. *J. Am. Chem. Soc.* **2016**, *138*, 13521–13524. [[CrossRef](#)] [[PubMed](#)]